Clinical Plasma Medicine 9 (2018) 34–40

Contents lists available at ScienceDirect

Clinical Plasma Medicine

journal homepage: www.elsevier.com/locate/cpme

Original research article

Permeabilization of human stratum corneum and full-thickness skin samples by a direct dielectric barrier discharge

Monika Gelker[a,b,*], Christel C. Müller-Goymann[b,c], Wolfgang Viöl[a]

[a] Department of Sciences and Technology, HAWK University of Applied Sciences and Arts, Von-Ossietzky-Str. 99, 37085 Göttingen, Germany
[b] PVZ – Center of Pharmaceutical Engineering, Technische Universität Braunschweig, Franz-Liszt-Str. 35a, 38106 Braunschweig, Germany
[c] Institut Pharmazeutische Technologie, Technische Universität Braunschweig, Mendelssohnstrasse 1, 38106 Braunschweig, Germany

ARTICLE INFO

Keywords:
Direct cold atmospheric plasma
Dielectric barrier discharge
Skin permeabilization
Transdermal drug delivery
Transepithelial electrical resistance
Franz cell permeation

ABSTRACT

Purpose: The tight barrier formed by human stratum corneum (SC) has a significantly protective function but also prevents the delivery of drug substances through the skin. In order to permeabilize the SC for drug delivery we use cold atmospheric plasma (CAP).

Methods: A direct *ex vivo* treatment of human skin with cold atmospheric plasma, specifically a dielectric barrier discharge (DBD) using skin as the ground electrode, was employed to permeabilize the stratum corneum (SC) throughout a treated area of 0.5 cm^2. The permeabilization of isolated SC and full-thickness skin was evaluated through changes in transepithelial electrical resistance. Franz diffusion cell permeation using differently sized hydrophilic particles enabled an estimation of the pore size and drug transport efficiency. Furthermore, silver sheet oxidation showed the distribution of local permeabilized regions.

Results: The transepithelial electrical resistance showed a long-term overall drop for treatments ≥ 90 s in isolated SC as well as full-thickness skin. Silver sheet oxidation revealed a regular pattern of local permeabilized regions greater in number than the expected number of skin appendages in treated isolated human SC. Permeation study results indicate that relatively small hydrophilic substances with Stokes' radii up to 1.4 nm are efficiently transported through human SC subsequent to 2×90 s treatment with direct cold atmospheric plasma at a power density of about 0.2 W cm^{-2}. A moderate permeation of particles up to 6 µm in diameter is evident for the occasional formation of large pores in the µm-range. Finally, a mechanism for DBD plasma permeabilization of skin is proposed and discussed.

1. Introduction

In human skin, the stratum corneum (SC) forms the air-liquid interface and is the foremost barrier against the penetration of potentially harmful substances from the outside and the loss of homeostasis within the body. This tight barrier is formed and continuously rebuilt by keratinocytes differentiating into tightly connected, rigid corneocytes. Consisting largely of keratin filaments and other tightly connected and cross-linked proteins, these dead cells are often described as the 'brick' surrounded by a 'mortar' of intercellular lipid lamellae in the SC-'wall' [1,2]. In human SC, 10–20 layers of corneocytes are stacked on top of each other and make up a layer of several micrometers, varying considerably in thickness between different body sites [3,4]. The lipid lamellae are organized into a highly ordered structure composed of stacked bilayers containing ceramides, cholesterol and free fatty acids in equal molar ratios [1]. Besides these effective and ever self-renewing barrier properties, the skin is a popular route for administering of small pharmaceuticals as it possesses several advantages over the two most important delivery routes, oral administration and hypodermic injection [5]. Transdermal drug delivery can make use of the natural 'soft spots' of the skin, namely hair follicles and their associated sebum glands or sweat ducts, which are collectively referred to as appendages. But often, drug delivery methods and vehicles try to overcome the SC itself as the appendages represent only a very small amount of the total skin surface (0.1%) and the intact SC does not facilitate permeation of molecules larger than 600 g mol^{-1}. Several methods to permeabilize the SC have been developed in the last decades. Among these are microneedle arrays, ablative techniques, sonophoresis and electroporation [6]. Many of these can be additionally combined with iontophoresis for directed diffusion.

Recently, a new method applying a technology referred to as cold atmospheric plasma (CAP) has been proposed. CAP, in brief, is a weakly ionized gas accompanied by reactive gas species, photons, as wells as electric fields and currents. It has recently received much attention for use in the

* Corresponding author at: Department of Sciences and Technology, HAWK University of Applied Sciences and Arts, Von-Ossietzky-Str. 99, 37085 Göttingen, Germany.
E-mail address: monika.gelker@hawk.de (M. Gelker).

https://doi.org/10.1016/j.cpme.2018.02.001
Received 12 January 2018; Accepted 6 February 2018

medical field [7]. Within the last decade, a multitude of plasma sources suitable for non-invasive application on living human skin have been developed and evaluated as to their operational safety, both physically and biologically [8–11]. By now, many CAP sources have been shown to be safe for use in patients [12,13] and several groups have used CAP to transfect cells in culture [14–20] or for transdermal drug delivery [21–24]. Together with the demonstrated potential of CAP for use in healing wounds [25–32] and treating inflammatory skin diseases [33], this technology is likely to play an increasingly important role in the medical field. As a prospective tool for drug delivery, CAP is thought to enhance the permeation of drugs which are highly potent (low dose needed) yet show high first-pass metabolism or are poorly soluble. In these cases, topical depot formation underneath the SC could be desirable.

The advantage of using CAP over, e.g., pure electroporation could lie in further synergistic effects of a CAP treatment, such as reduction in bacterial load [34,35], increase in microcirculation [36,37] or skin acidification [38] in the treatment of skin diseases. Recent studies with plasma jet systems have proposed skin regenerating effects [39] and a benefit of plasma treatment in the treatment of atopic dermatitis [40].

2. Materials and methods

2.1. Skin and stratum corneum preparation

Skin samples were obtained from patients undergoing abdominal plastic surgery (Department of Trauma-, Orthopaedic- and Plastic Surgery, University Medical Center Göttingen, Germany). All donors gave their oral and written informed consent prior to the procedure and the experiments were performed according to the Declaration of Helsinki principles following ethics committee approval.

The stratum corneum (SC) was prepared according to Kligman and Christophers [41] as in Täuber and Müller-Goymann [42]. Briefly, skin donations were collected immediately after the surgery, subcutaneous fat was removed and the skin was frozen in liquid nitrogen or a − 80 °C solid coolant to be stored subsequently at − 20 °C. For full-thickness skin (FTS) experiments, however, 15 mm circles were punched out of the freshly prepared skin and immediately employed in the permeation experiments. For SC isolation, thawed samples were subjected to 48 h of trypsinization at 37 °C with 50 mg trypsin (Carl Roth GmbH, Karlsruhe, Germany) per 100 mL tap water. After washing and air-drying, the SC was stored in a desiccator and used within 3 months. For permeabilization studies, circles of 15 mm were punched out. As shown in Fig. 1B/C, the autofluorescence of the SC was used to characterize the samples by laser-scanning microscopy (LSM 700, Carl Zeiss AG, Oberkochen, Germany). The hydrated SC showed the characteristic polygonal structure of the corneocytes and a mean thickness of 9.1 ± 3.9 µm was calculated from the cut projections of 3D images.

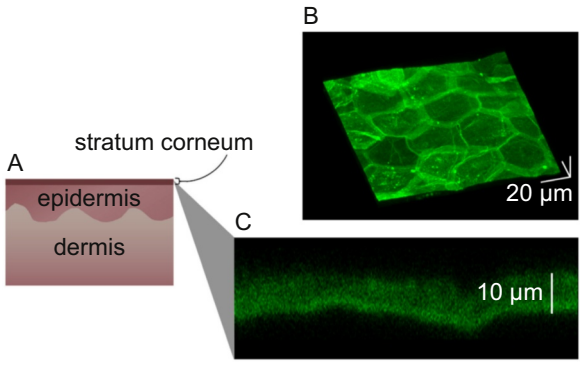

Fig. 1. (A) Diagram of full thickness skin. Autofluorescence of hydrated stratum corneum permits 3D imaging via laser-scanning microscopy (excitation at 488 nm). The 3D projection (B) shows the characteristic polygonal shape of corneocytes (20× objective). The scale bar indicates 20 µm in all dimensions. (C) The thickness was measured from cut projections of image stacks captured with a 50× objective.

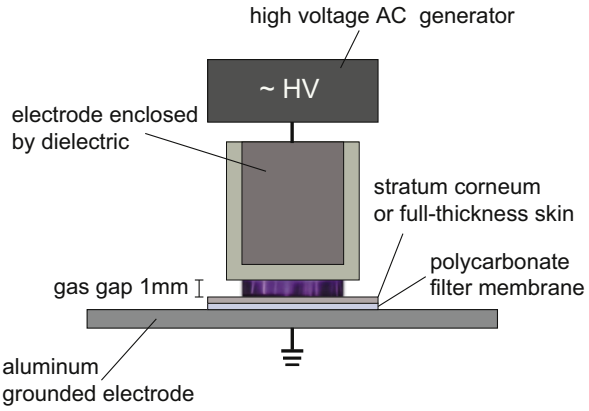

Fig. 2. Setup for cold atmospheric plasma treatment of isolated stratum corneum or full-thickness skin.

2.2. Cold atmospheric plasma treatment

For the cold atmospheric plasma treatment of isolated SC or FTS, a direct barrier discharge (DBD) arrangement (volume mode) in ambient air was operated with a gas gap of 1 mm (see Fig. 2). This plasma source, sometimes referred to as direct cold atmospheric plasma (diCAP), was operated with alternating high voltage pulses of 70 µs duration at a constant repetition rate of 300 Hz and has been extensively described elsewhere [43]. The 8 mm high voltage electrode was enclosed by an Al_2O_3 ceramic cup with 10 mm outer diameter and a 1 mm wall thickness serving as the dielectric. Using this electrode, a SC or FTS area of 0.5 cm^2 was treated for a duration of 90 s or 2 × 90 s with an intermittent pause of 10 min. The applied power density was measured to be 212 ± 20 mW cm^{-2} for SC and 222 ± 19 mW cm^{-2} for FTS. Consequently, the energy density amounted to 19.1 ± 1.8 J cm^{-2} or 38.2 ± 3.6 J cm^{-2} for SC and 20.0 ± 1.7 J cm^{-2} or 40.0 ± 3.4 J cm^{-2} for FTS.

2.3. Electrolytic imaging of permeabilization

In order to visualize the zones of decreased electrical resistance and evaluate the distribution of these zones across the CAP-treated SC surface, an electrolytic reaction was applied [44]. The treated SC was positioned between a square silver plate and a PBS-agarose gel disc (0.5 cm thickness, 2%) and these were connected to the positive and negative electrodes of a weak voltage source (8.5 V) as illustrated in Fig. 3. The agarose disc needed to be smaller than the SC to avoid bypass pathways from forming around the SC and the gel was prepared with 2% agarose in phosphate-buffered saline. Discs of 12 mm diameter were punched out before use. Throughout the experiments, an electric voltage of 8.5 V was applied for 10 s to all samples. The resulting current flow took values between the detection limit (1 µA cm^{-2}) for untreated SC and 1 mA cm^{-2} for CAP-treated SC specimen. The agarose disc and SC were consecutively removed from the silver sheet. At regions with low resistance, AgCl had formed on the surface of the silver plate from electrochemically formed Ag^+ ions and diffusing Cl^- ions. This 'resistivity map' [45] darkened when exposed to the surrounding air and the treated area was imaged on an Axio Imager Z.2 system with an Axiocam 105

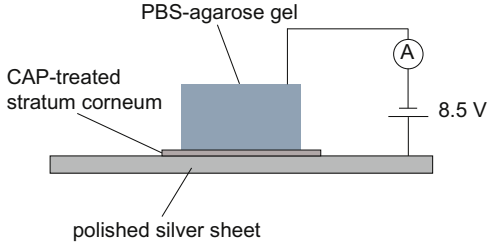

Fig. 3. Setup for electrolytic imaging of permeabilized regions after CAP treatment.

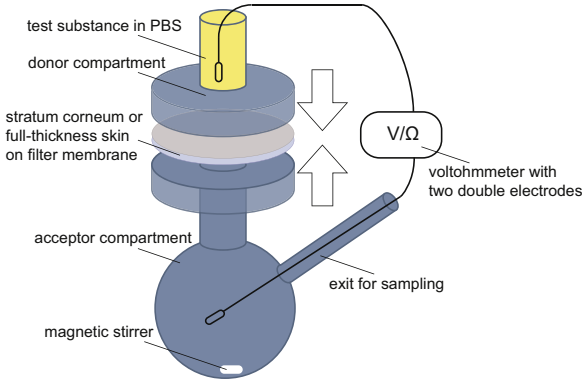

Fig. 4. Modified Franz diffusion cell setup including positioning of the electrodes for transepithelial electrical resistance (TEER) measurements.

color camera (Carl Zeiss AG, Oberkochen, Germany) and a 10× objective (Plan-Neofluar, NA 0.3) in the 'tiles' mode, which stitched together 206 individual images to display the whole area of interest.

2.4. Permeation studies with modified Franz diffusion cells

The permeation of various fluorescent test substances was tested with and without prior CAP treatment through isolated SC or fresh FTS as the barrier. Experiments with modified Franz diffusion cells [46] were conducted as described in detail by Täuber and Müller Goymann [42] as well as Lusiana et al. [47]:

Prior to any experiment isolated SC was tested for its integrity against bright light, briefly hydrated in deionized water and subsequently handled with the help of a polycarbonate membrane filter (Isopore®, Merck KGaA, Darmstadt, Germany) with 5 µm pores and a diameter of 15 mm underneath the SC. The filter did not constitute a diffusion barrier for substances up to 2 µm in diameter. For 6 µm particles a polyester mesh fabric was used as a stabilizing membrane.

After CAP treatment, the SC and membrane filter were fixed between the siliconized donor and receiver compartments of the modified Franz diffusion cell (Fig. 4). The acceptor chamber was filled with 32 °C phosphate-buffered saline (PBS, pH 7.4) which had been autoclaved and vacuum-degassed beforehand to avoid bubble formation. The acceptor volumes varied between 4.46 mL and 5.91 mL for different cells. The donor compartment was filled with 500–1000 µL of PBS containing one of the test substances (see Table 1). All substances used were hydrophilic and fluorescent. Fluorescein and the FITC-labeled dextrans were obtained from Merck KGaA (Darmstadt, Germany); the nano- and microparticles were Fluoresbrite® Fluorescent carboxylated polystyrene microspheres (Polyscience Inc., Warrington, USA). They were chosen to cover a wide range of sizes in order to evaluate the pore size obtained by CAP treatment. The donor compartments and sample ports were sealed with Parafilm® M to avoid spilling and evaporation as was the donor-acceptor junction to avoid diffusion of liquids into and out of the diffusion cell. Calculated from the minimum diameter of donor and acceptor compartment openings, the permeation area ranged between 0.44 cm^2 and 0.55 cm^2.

During permeation experiments all Franz diffusion cells were incubated at 32 °C in a water bath and stirred at 300 rpm. Samples of 100 µL or 250 µL, depending on the test substance were taken after 30 min, 2 h, 12 h and 24 h and the volume was directly replaced by warm PBS. The samples were stored in the dark at room temperature in an opaque 96-well plate (Nunc AS, Roskilde, Denmark). Fluorescence intensities were measured with one of two fluorescence plate readers Victor (PerkinElmer Inc., Waltham, USA) or Tristar2S (Berthold Technologies, Bad Wildbad, Germany) with excitation at 485 nm. Emitted fluorescent light was detected at 535 nm. Calibration samples were prepared in PBS from an aliquot of the donor solution. The calibration curves covered the entire range of intensities displayed by the permeation samples.

Experiments with FTS followed the same procedure and so far only fluorescein was used as a model drug. The samples used were donated skin from the buttocks of a 45-year-old female (No. 4) and abdominal skin from a 46-year-old female (No. 5).

2.5. Measurement of transepithelial electrical resistance (TEER)

Concurrent with permeation studies, the transepithelial electrical resistance (TEER) across plasma-treated SC or FTS was measured during the Franz cell permeation experiments to evaluate the degree of permeabilization generated through cold atmospheric plasma treatment. Similar to Fokuhl and Müller-Goymann [48], who used TEER measurements to test isolated SC for integrity, a voltohmmeter (EVOM2 with extended range, World Precision Instruments, Sarasota, USA) with custom-made Ag/AgCl electrodes and a measurement range from 10 Ω to 120 kΩ was used. One electrode pair was inserted into the donor compartment of the modified Franz diffusion cell and the other electrode pair introduced into the acceptor compartment through the sample port. For intact SC the TEER usually reached or exceeded the maximum range around 120 kΩ, which corresponds to a maximum value of 60 kΩ cm^2 when an area of 0.5 cm^2 is examined. The blank value for the electrical resistance in this configuration (with the filter membrane but without SC) was determined to be 0.3 kΩ.

2.6. Statistical analysis

All data in this study are expressed as the arithmetic mean ± SD unless noted otherwise. Permeation experiments were usually performed at least three times (twice for fluorescein and 6 µm particles) and included four samples in each group for every experiment. Statistical analysis was performed using one-way ANOVA with the Bonferroni correction of p-values for post-hoc tests in Origin 2017G (OriginLab, Northampton, USA). Statistical significance was determined at $\alpha = 0.05$.

As extreme outliers, individual data points were excluded from the calculations in cases where the values exceeded the next highest value by more than a factor of ten (only necessary for FITC-dextran 40 kDa).

Correlation was evaluated in IBM SPSS Statistics 24 (IBM Corp., Armonk, USA) using the Spearman's rank correlation coefficient as a nonparametric measure of correlation.

3. Results and discussion

In recent years, plasma permeabilization of skin has been shown to be feasible in mice [21], for pig skin [22] and for human skin [49] using jet systems. A dielectric barrier discharge (DBD) realized as a 'microplasma'

Table 1
Substances used for permeation experiments.

substance	acronym	MW (g mol^{-1})	radius (nm)	amount in donor compartment (µg)	sample size (µL)	skin donor (No., sex, age)
Fluorescein	–	332	–	500	100	1, female, 46
FITC-dextran 4	FD4	4000	[a]1.4	1000	100	1, female, 46
FITC-dextran 40	FD40	40,000	[a]4.5	1000	100	2, female, 47
FITC-dextran 500	FD500	500,000	[a]14.7	1000	100	2, female, 47
500 nm particles	500 nm	–	250	125	250	2, female, 47
2 µm particles	2 µm	–	1000	250	250	3, male, 55
6 µm particles	6 µm	–	3000	250	250	3, male, 55

[a] Stokes' radius according to supplier.

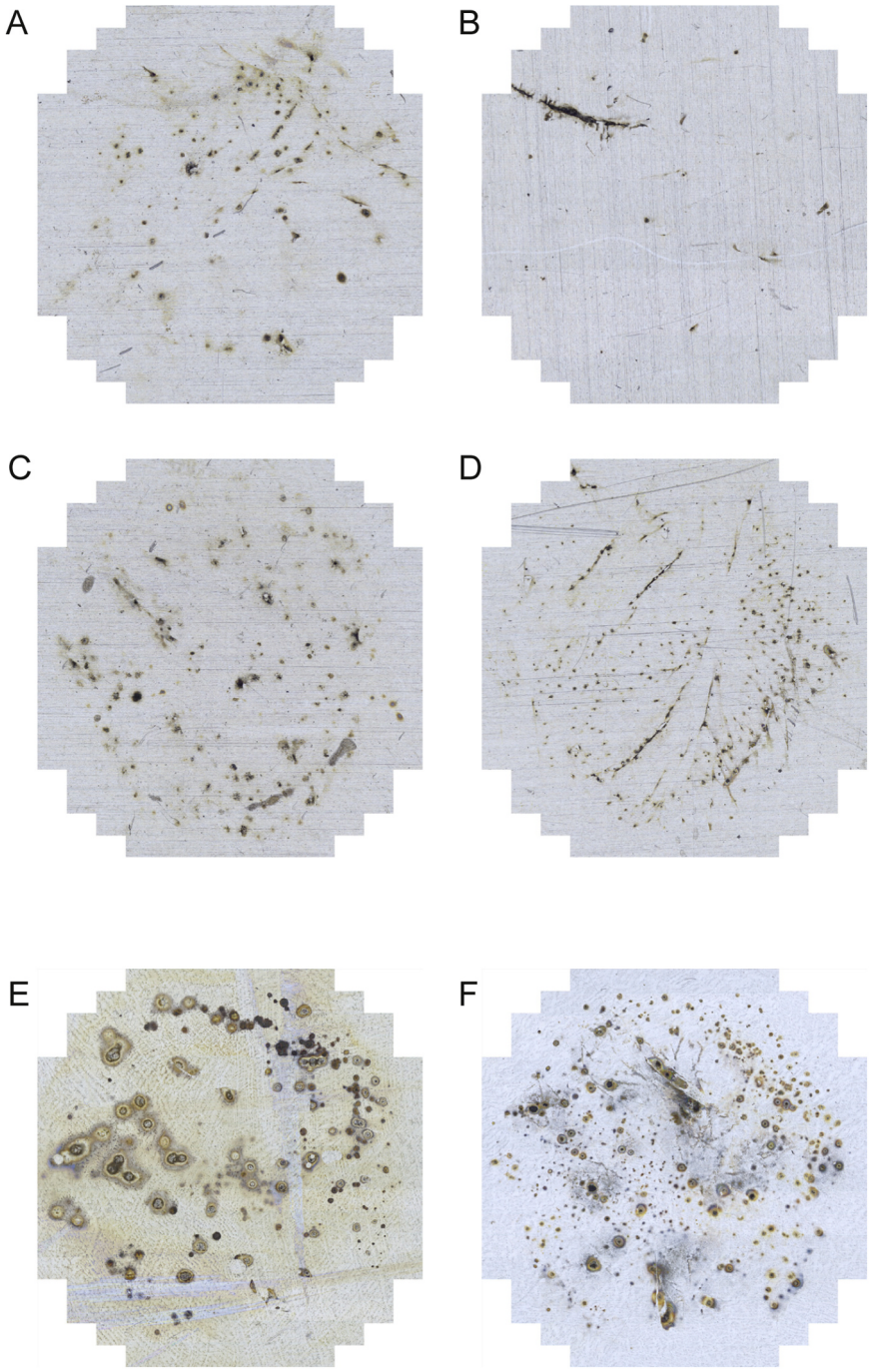

Fig. 5. Electrodeposition of AgCl on polished silver sheets 30 min after plasma treatment for 1 × 90 s (A, B) or 2 × 90 s (C, D). Two representative images are shown for each treatment duration. Long-term permeabilization is shown for the same sample 3 h (E) and 24 h (F) after the CAP treatment for 2 × 90 s. Individual image dimensions are 10.5 × 10.9 mm for all six images.

film electrode has been shown to permeabilize the skin of Yucatan micropigs [24]. But this study, to our knowledge, is the first to show permeabilization of human skin with a DBD that uses skin as the ground electrode for discharge formation. The methods employed here complement each other to form a coherent picture of the capabilities of a direct cold atmospheric plasma (CAP) treatment to modify the human skin barrier properties in both model systems, isolated stratum corneum (SC) and full-thickness skin (FTS).

When operated on human skin the discharge is filamentary in appearance [50]. The stochastically occurring filaments and those formed due to surface irregularities (e.g. small hairs) represented regions of relatively high air-ionization and current flow.

After one or two 90 s CAP treatments of human stratum corneum, the electrolytic oxidation of a silver sheet below treated SC reveals punctiform zones of decreased electrical resistance as darkening spots of AgCl (Fig. 5). The permeabilized regions form throughout the treated area of 0.5 cm^2. They vary in size and number from treatment to treatment. In intact, untreated SC as a control, the voltage employed did not lead to any meaningful flow of current across the skin and no darkened zones were visible on the control silver sheets afterwards (data not shown).

Since a very similar effect and pattern was shown for skin permeabilization by electric fields by Pliquett et al. [44,45], these results suggest that a similar mechanism is at work during plasma permeabilization in this study.

Because a constant voltage source is used for the electrolytic imaging, the degree of permeabilization reached through CAP treatment already becomes obvious by an increased current flow across the stratum corneum

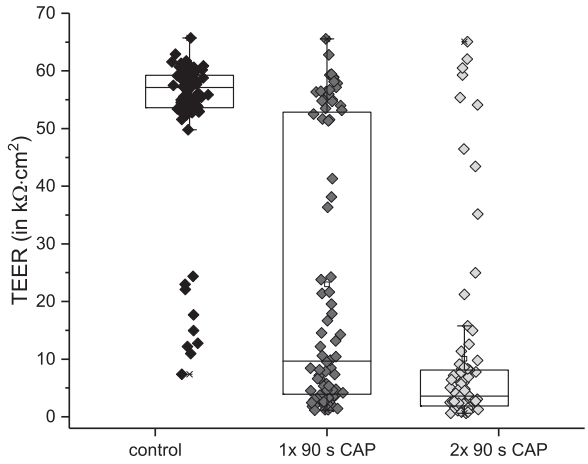

Fig. 6. Collected transepithelial electrical resistance (TEER) values from all permeation experiments through isolated SC treated with cold atmospheric plasma (CAP). SC was CAP-treated for 1 × or 2 × 90 s, or left untreated (control). TEER was measured 24 h after the treatment. Individual data points and box plots indicate the median, 25% and 75% percentiles. Each group contains 81–84 SC samples. Differences between all groups are highly significant ($p \ll 0.001$).

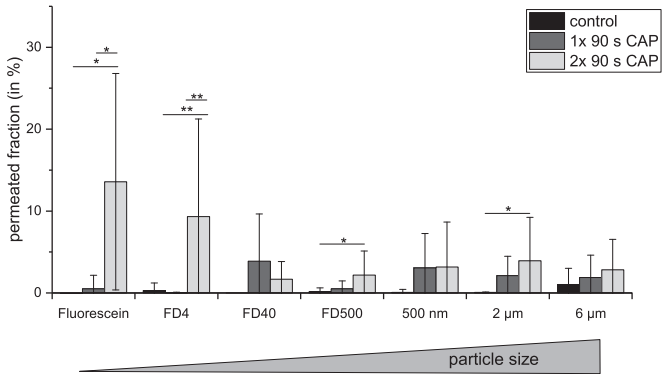

Fig. 7. Permeated fractions of various test substances and particles differing in size (see Table 1 for details) after 24 h of Franz cell permeation. Values are given for SC, which was CAP-treated for 1 × or 2 × 90 s, or left untreated (control). (*) $p < 0.05$; (**) $p < 0.01$. Substance abbreviations: FD4 – FITC-dextran 4000 g mol^{-1}; FD40 – FITC-dextran 40,000 g mol^{-1}; FD500 – FITC-dextran 500,000 g mol^{-1}.

Table 2
Correlation of permeated amount of test substances with SC electrical conductance 24 h after plasma treatment. The correlation is significant ($p < 0.01$).

Substance	Correlation coefficient
Fluorescein	0,881
FITC-dextran 4	0,764
FITC-dextran 40	0,846
FITC-dextran 500	0,657
500 nm particles	0,711
2 µm particles	0,768
6 µm particles	0,566

during electrolysis. While intact SC with a high electrical resistance will permit a current flow of no more than 1 µA cm^{-2}, the detection limit of the employed ampere meter, the electrical current rises to up to 1 mA cm^{-2} after two 90 s CAP treatments. The SC permeabilization was shown to be largely irreversible, since in the very same SC sample, zones of lowered electrical resistance were visualized 3 h and 24 h after a CAP treatment (Fig. 5 B).

The electrical properties of CAP-treated skin were evaluated in more detail and over prolonged periods during permeation experiments. Fig. 6 shows a robust effect of CAP treatment on the transepithelial electrical resistance (TEER) measured 24 h after the treatment. While intact SC, constituting the main barrier of the skin, possesses a very high TEER of > 50 kΩ cm^2, the resistance decreases dramatically upon CAP treatment for 90 s to a mean value of 23 kΩ cm^2. Despite this clear trend, it has to be noted, that the distribution of SC resistance values for a 90 s treatment was of a bimodal nature; most samples show a strong drop in TEER, but a non-negligible share of samples appears to be unchanged after a single treatment. Measurements from samples that had been treated twice for 90 s with a 10 min intermittent pause were distributed more evenly. The overwhelming majority of double treated SC displayed a very low TEER below 10 kΩ cm^2 (arithmetic mean: 10 ± 16 kΩ cm^2).

Whereas the previously described methods serve to illustrate the electrical current flow and the permeation of small ions through CAP-treated SC, the Franz cell permeation studies further explore the treated SC with regard to the size of substances and particles that would be able to penetrate the skin after CAP application. To this end, substances ranging from the relatively small hydrophilic fluorescein (332 g mol^{-1}) via FITC-labeled dextran molecules (Stokes' radii from 1.4 to 14.8 nm) to polystyrene particles with diameters of up to 6 µm were used as donor substances. As summarized in Fig. 7, the fraction of donor substance passing through CAP-treated SC within 24 h was related to the particle size in an inversely proportional way. Large fractions of relatively small substances with a Stokes' radius of up to 1.4 nm were able to pass through plasma-treated SC. For larger hydrophilic components from approx. 9 nm to 6 µm in diameter, permeation is improved after 2 × 90 s CAP treatment as often as not. This indicates that the pores or defects formed upon plasma treatment, as already suggested by silver oxidation images shown above, are not of uniform size but may differ from sample to sample as well as within a single sample and may reach dimensions in the µm-scale *ex vivo*.

The permeation of test substances may successfully be connected to the TEER values measured during the same experiments through non-parametric correlation testing. A statistically significant ($p < 0.01$) positive correlation of the permeated amount of donor substance after 24 h with the conductance value (reciprocal of the TEER) was found for all seven donor substances (Table 2).

Finally yet importantly, plasma permeabilization by CAP treatment was successfully shown for full thickness skin (FTS) as illustrated in Fig. 8. Even more pronounced than in isolated SC, the TEER value robustly and dramatically decreased within a few minutes of the CAP treatment and remained at this level for the entire 48 h of an experiment. As one would have expected, the fraction of fluorescein passing through human skin (including full epidermis and dermis) was much lower than for isolated SC. However, a CAP treatment for 2 × 90 s increased the mean amount of permeated fluorescein after 48 h by a factor of 18. It may be hypothesized that a much higher amount of fluorescein penetrated into the skin without being released at the acceptor site and this will be the subject of further studies.

The mechanism of skin permeabilization through CAP treatment is likely to be similar to that of electroporation. In this context, the electric field and electric currents occurring during the gas discharges are expected to play a major role in the formation of aqueous pores in the SC. At present it cannot be excluded that the sites of permeabilization colocalize with appendages such as sweat ducts. However, the abdominal density of sweat ducts in European males has been reported to be approx. 1 per mm^2 [51]. This would correspond to a number of 50 sites on average in the sample area of 0.5 cm^2 treated in this study. Because the density of ion transport regions (Fig. 5) was observed to be more than 200 per 0.5 cm^2, well exceeding the density of skin sweat ducts, we hypothesize that pathways form within the 'bricks and mortar' of the SC, most likely in an intercellular mode as shown for electroporation [52]. We correspondingly propose that electroporation followed by 'joule heating' in regions of high 'plasma density'– meaning the filaments in the discharge volume – is responsible for the observed permeabilization [45]. This would mean that when the phase transition temperature (several are reported; a major melting temperature is 65 °C [53]) is reached, the highly ordered structure of the lipid bilayers is transformed and reshaped into a less impermeable organization that should be further elucidated. In electroporation, the partly irreversible formation of vesicular structures has been shown and attributed to Joule heating [45]. Since the gas temperature

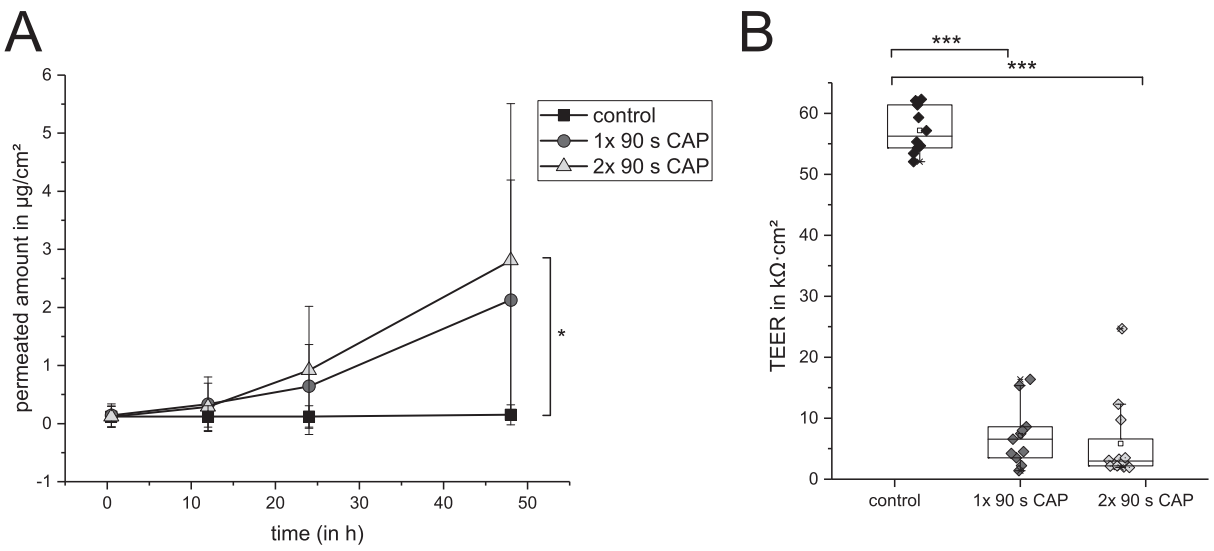

Fig. 8. (A) Franz diffusion cell permeation of fluorescein through full-thickness skin. Skin samples received cold atmospheric plasma (CAP) exposure for 1 × 90 s, 2 × 90 s or were left untreated (control). (*) $p < 0.05$. (B) Transepithelial electrical resistance (TEER) values from full-thickness skin permeation experiments recorded 24 h after CAP treatment. (***) $p < 0.001$.

of the discharge used in this study has been estimated to lie at 375 ± 50 K, it is possible that the phase transition of skin lipids is triggered in CAP treatment. However, no bulk heating of skin or SC has been observed in infrared camera images (unpublished data). Therefore this is likely to happen where a filament occurs. Furthermore, simulations have recently shown that lipid oxidation, which is likely to occur in CAP-treated skin through reactive species formed in the discharge volume, may facilitate permeabilization of the skin by reducing the electric field threshold for pore formation [54]. This indicates a synergistic effect of several components from the CAP working together for a long-lasting permeabilization of human skin. Of course the feasibility has yet to be shown *in vivo*. This is especially relevant in view of previous studies that showed a permeabilization of skin *ex vivo*, which could not be reproduced *in vivo* [55].

4. Conclusion

A CAP treatment in isolated human SC was shown to dramatically reduce electrical resistance and yield a regular pattern of locally permeabilized regions. These regions were greater in number than the natural number of skin appendages and admitted the passage of small hydrophilic substances with Stokes' radii up to 1.4 nm through human SC subsequent to 2 × 90 s CAP treatment. Proof-of-principle experiments with full-thickness skin (FTS) confirm these results. The occasional formation of large pores in the µm-range was so far observed in isolated SC only and should be studied in FTS in the future as it might increase the risk of infection through bacteria penetration. A mechanism for plasma permeabilization is proposed that is similar to the permeabilization of human skin by electric fields. In addition to the hydrophilic substances tested for permeation so far, future experiments will also include lipophilic components or formulations to increase the relevance of this method for drug delivery purposes.

In recent years, both the fields of medical use of CAP and research into cutaneous drug delivery systems have grown, but to date little is known about underlying mechanisms. With this study we hope to contribute to a better understanding of the mechanisms by which cold atmospheric plasmas, and specifically direct discharges using the biological tissue as a counter electrode, interact with the human body.

Acknowledgements

The authors would like to thank Dr. Jennifer Ernst and Dr. Gunther Felmerer at the Department of Trauma-, Orthopaedic- and Plastic Surgery of the University Medical Center Göttingen for their continued help with the provision of donated skin and Astrid Ichter her for support with permeation experiments. The expert introduction to SC preparation and permeation experiments by Dr. Anja Täuber as well as helpful discussions with Prof. Dr. Uwe Pliquett concerning electrolytic imaging of permeation and the mechanism of skin electroporation are gratefully acknowledged. Thanks are also due to Dr. Andreas Helmke for his helpful discussion and Roger Skarsten for proof-reading of the manuscript.

Funding

This research was funded by a Georg-Christoph-Lichtenberg grant to Monika Gelker through the PhD Program *Processing of poorly soluble drugs at small scale*, funded by Lower Saxony's Ministry of Science and Culture (MWK). Experimental equipment is funded by the Federal Ministry of Education and Research through the research project PlasBaWirk (FKZ: 03FH015IX5).

Conflict of interest

The authors declare no conflict of interest.

Ethical statement

Skin samples were obtained from patients undergoing abdominal plastic surgery (Department of Trauma-, Orthopaedic- and Plastic Surgery, University Medical Center Göttingen, Germany). All donors gave their oral and written informed consent and were given the opportunity to ask questions prior to the procedure. The experiments were performed according to the Declaration of Helsinki principles following ethics committee approval.

References

[1] T. Matsui, M. Amagai, Dissecting the formation, structure and barrier function of the stratum corneum, Int. Immunol. 27 (6) (2015) 269–280.
[2] Z. Nemes, P.M. Steinert, Bricks and mortar of the epidermal barrier, Exp. Mol. Med. 31 (1) (1999) 5–19.
[3] M. Egawa, T. Hirao, M. Takahashi, In vivo estimation of stratum corneum thickness from water concentration profiles obtained with Raman spectroscopy, Acta Derm. Venereol. 87 (1) (2007) 4–8.
[4] H. Tagami, Location-related differences in structure and function of the stratum corneum with special emphasis on those of the facial skin, Int. J. Cosmet. Sci. 30 (6) (2008) 413–434.
[5] M.R. Prausnitz, R. Langer, Transdermal drug delivery, Nat. Biotechnol. 26 (11)

(2008) 1261–1268.
[6] B.W. Barry, Novel mechanisms and devices to enable successful transdermal drug delivery, Eur. J. Pharm. Sci. 14 (2) (2001) 101–114.
[7] D. Graves, S. Hamaguchi, D. O'Connell, In focus: plasma medicine, Biointerphases 10 (2) (2015) 29301.
[8] C. Welz, S. Becker, Y.-F. Li, T. Shimizu, J. Jeon, S. Schwenk-Zieger, H.M. Thomas, G. Isbary, G.E. Morfill, U. Harréus, J.L. Zimmermann, Effects of cold atmospheric plasma on mucosal tissue culture, J. Phys. D: Appl. Phys. 46 (4) (2013) 45401.
[9] G. Isbary, J. Köritzer, A. Mitra, Y.-F. Li, T. Shimizu, J. Schroeder, J. Schlegel, G.E. Morfill, W. Stolz, J.L. Zimmermann, Ex vivo human skin experiments for the evaluation of safety of new cold atmospheric plasma devices, Clin. Plasma Med. 1 (1) (2013) 36–44.
[10] R. Tiede, J. Hirschberg, G. Daeschlein, T. von Woedtke, W. Vioel, S. Emmert, Plasma applications: a dermatological view, Contrib. Plasma Phys. 54 (2) (2014) 118–130.
[11] T. Maisch, A.K. Bosserhoff, P. Unger, J. Heider, T. Shimizu, J.L. Zimmermann, G.E. Morfill, M. Landthaler, S. Karrer, Investigation of toxicity and mutagenicity of cold atmospheric argon plasma, Environ. Mol. Mutagen. 58 (3) (2017) 172–177.
[12] T. von Woedtke, S. Reuter, K. Masur, K.-D. Weltmann, Plasmas for medicine, Phys. Rep. 530 (4) (2013) 291–320.
[13] Y. Setsuhara, Low-temperature atmospheric-pressure plasma sources for plasma medicine, Arch. Biochem. Biophys. 605 (2016) 3–10.
[14] Y. Ogawa, N. Morikawa, A. Ohkubo-Suzuki, S. Miyoshi, H. Arakawa, Y. Kita, S. Nishimura, An epoch-making application of discharge plasma phenomenon to gene-transfer, Biotechnol. Bioeng. 92 (7) (2005) 865–870.
[15] Y. Sakai, V. Khajoee, Y. Ogawa, K. Kusuhara, Y. Katayama, T. Hara, A novel transfection method for mammalian cells using gas plasma, J. Biotechnol. 121 (3) (2006) 299–308.
[16] R.J. Connolly, J.I. Rey, V.M. Lambert, G. Wegerif, M.J. Jaroszeski, K.E. Ugen, Enhancement of antigen specific humoral immune responses after delivery of a DNA plasmid based vaccine through a contact-independent helium plasma, Vaccine 29 (39) (2011) 6781–6784.
[17] C.M. Edelblute, L.C. Heller, M.A. Malik, R. Heller, Activated air produced by shielded sliding discharge plasma mediates plasmid DNA delivery to mammalian cells, Biotechnol. Bioeng. 112 (12) (2015) 2583–2590.
[18] Y. Ikeda, H. Motomura, Y. Kido, S. Satoh, M. Jinno, Effects of molecular size and chemical factor on plasma gene transfection, Jpn. J. Appl. Phys. 55 (7S2) (2016) 07LG06.
[19] M. Jinno, Y. Ikeda, H. Motomura, Y. Isozaki, Y. Kido, S. Satoh, Synergistic effect of electrical and chemical factors on endocytosis in micro-discharge plasma gene transfection, Plasma Sources Sci. Technol. 26 (6) (2017) 65016.
[20] M. Leduc, D. Guay, R.L. Leask, S. Coulombe, Cell permeabilization using a non-thermal plasma, N. J. Phys. 11 (11) (2009) 115021.
[21] R.J. Connolly, G.A. Lopez, A.M. Hoff, M.J. Jaroszeski, Plasma facilitated delivery of DNA to skin, Biotechnol. Bioeng. 104 (5) (2009) 1034–1040.
[22] O. Lademann, H. Richter, M.C. Meinke, A. Patzelt, A. Kramer, P. Hinz, K.-D. Weltmann, B. Hartmann, S. Koch, Drug delivery through the skin barrier enhanced by treatment with tissue-tolerable plasma, Exp. Dermatol. 20 (6) (2011) 488–490.
[23] J.-H. Choi, S.-H. Nam, Y.-S. Song, H.-W. Lee, H.-J. Lee, K. Song, J.-W. Hong, G.-C. Kim, Treatment with low-temperature atmospheric pressure plasma enhances cutaneous delivery of epidermal growth factor by regulating E-cadherin-mediated cell junctions, Arch. Dermatol. Res. 306 (7) (2014) 635–643.
[24] K. Shimizu, K. Hayashida, M. Blajan, Novel method to improve transdermal drug delivery by atmospheric microplasma irradiation, Biointerphases 10 (2) (2015) 29517.
[25] G. Lloyd, G. Friedman, S. Jafri, G. Schultz, A. Fridman, K. Harding, Gas plasma: medical uses and developments in wound care, Plasma Process. Polym. 7 (3–4) (2010) 194–211.
[26] H.-R. Metelmann, T.T. Vu, H.T. Do, T.N.B. Le, T.H.A. Hoang, T.T.T. Phi, T.M.L. Luong, V.T. Doan, T.T.H. Nguyen, T.H.M. Nguyen, T.L. Nguyen, D.Q. Le, T.K.X. Le, T. von Woedtke, R. Bussiahn, K.-D. Weltmann, R. Khalili, F. Podmelle, Scar formation of laser skin lesions after cold atmospheric pressure plasma (CAP) treatment: a clinical long term observation, Clin. Plasma Med. 1 (1) (2013) 30–35.
[27] G. Isbary, J.L. Zimmermann, T. Shimizu, Y.-F. Li, G.E. Morfill, H.M. Thomas, B. Steffes, J. Heinlin, S. Karrer, W. Stolz, Non-thermal plasma—more than five years of clinical experience, Clin. Plasma Med. 1 (1) (2013) 19–23.
[28] S. Emmert, F. Brehmer, H. Hänßle, A. Helmke, N. Mertens, R. Ahmed, D. Simon, D. Wandke, W. Maus-Friedrichs, G. Däschlein, M.P. Schön, W. Viöl, Atmospheric pressure plasma in dermatology: Ulcus treatment and much more, Clin. Plasma Med. 1 (1) (2013) 24–29.
[29] S. Arndt, P. Unger, E. Wacker, T. Shimizu, J. Heinlin, Y.-F. Li, H.M. Thomas, G.E. Morfill, J.L. Zimmermann, A.-K. Bosserhoff, S. Karrer, M. Hamblin, Cold atmospheric plasma (CAP) changes gene expression of key molecules of the wound healing machinery and improves wound healing in vitro and in vivo, PLoS One 8 (11) (2013) e79325.
[30] B. Haertel, T. von Woedtke, K.-D. Weltmann, U. Lindequist, Non-thermal atmospheric-pressure plasma possible application in wound healing, Biomol. Ther. 22 (6) (2014) 477–490.
[31] D. Lendeckel, C. Eymann, P. Emicke, G. Daeschlein, K. Darm, S. O'Neil, A.G. Beule, T. von Woedtke, U. Völker, K.-D. Weltmann, M. Jünger, W. Hosemann, C. Scharf, Proteomic changes of tissue-tolerable plasma treated airway epithelial cells and their relation to wound healing, BioMed. Res. Int. 2015 (2015) 1–17.
[32] F. Brehmer, H.A. Haenssle, G. Daeschlein, R. Ahmed, S. Pfeiffer, A. Görlitz, D. Simon, M.P. Schön, D. Wandke, S. Emmert, Alleviation of chronic venous leg ulcers with a hand-held dielectric barrier discharge plasma generator (PlasmaDerm ® VU-2010): results of a monocentric, two-armed, open, prospective, randomized and controlled trial (NCT01415622), J. Eur. Acad. Dermatol. Venereol. 29 (1) (2015) 148–155.
[33] J.-H. Choi, Y.-S. Song, H.-J. Lee, J.-W. Hong, G.-C. Kim, Inhibition of inflammatory reactions in 2,4-Dinitrochlorobenzene induced Nc/Nga atopic dermatitis mice by non-thermal plasma, Sci. Rep. 6 (2016) 27376.
[34] R. Laurita, A. Miserocchi, M. Ghetti, M. Gherardi, A. Stancampiano, V. Purpura, D. Melandri, P. Minghetti, E. Bondioli, V. Colombo, Cold atmospheric plasma treatment of infected skin tissue: evaluation of sterility, viability, and integrity, IEEE Trans. Radiat. Plasma Med. Sci. 1 (3) (2017) 275–279.
[35] A. Helmke, D. Hoffmeister, F. Berge, S. Emmert, P. Laspe, N. Mertens, W. Vioel, K.-D. Weltmann, Physical and microbiological characterisation of Staphylococcus epidermidis inactivation by dielectric barrier discharge plasma, Plasma Process. Polym. 8 (4) (2011) 278–286.
[36] T. Kisch, A. Helmke, S. Schleusser, J. Song, E. Liodaki, F.H. Stang, P. Mailaender, R. Kraemer, Improvement of cutaneous microcirculation by cold atmospheric plasma (CAP): results of a controlled, prospective cohort study, Microvasc. Res. 104 (2016) 55–62.
[37] T. Borchardt, J. Ernst, A. Helmke, M. Tanyeli, A.F. Schilling, G. Felmerer, W. Viöl, Effect of direct cold atmospheric plasma (diCAP) on microcirculation of intact skin in a controlled mechanical environment, Microcirculation 24 (8) (2017).
[38] A. Helmke, D. Hoffmeister, N. Mertens, S. Emmert, J. Schuette, W. Vioel, The acidification of lipid film surfaces by non-thermal DBD at atmospheric pressure in air, N. J. Phys. 11 (11) (2009) 115025.
[39] J.H. Choi, Y.S. Song, K. Song, H.J. Lee, J.W. Hong, G.C. Kim, Skin renewal activity of non-thermal plasma through the activation of β-catenin in keratinocytes, Sci. Rep. 7 (1) (2017) 6146.
[40] J.-H. Choi, Y.-S. Song, H.-J. Lee, G.-C. Kim, J.-W. Hong, The topical application of low-temperature argon plasma enhances the anti-inflammatory effect of Jaun-ointment on DNCB-induced NC/Nga mice, BMC Complement. Altern. Med. 17 (1) (2017) 340.
[41] A.M. Kligman, E. Christophers, Preparation of isolated sheets of human stratum corneum, Arch. Dermatol. 88 (1963) 702–705.
[42] A. Täuber, C.C. Müller-Goymann, In vitro permeation and penetration of ciclopirox olamine from poloxamer 407-based formulations–comparison of isolated human stratum corneum, bovine hoof plates and keratin films, Int. J. Pharm. 489 (1–2) (2015) 73–82.
[43] J. Hirschberg, T. Omairi, N. Mertens, A. Helmke, S. Emmert, W. Viöl, Influence of excitation pulse duration of dielectric barrier discharges on biomedical applications, J. Phys. D: Appl. Phys. 46 (16) (2013) 165201.
[44] U.F. Pliquett, T.E. Zewert, T. Chen, R. Langer, J.C. Weaver, Imaging of fluorescent molecule and small ion transport through human stratum corneum during high voltage pulsing: localized transport regions are involved, Biophys. Chem. 58 (1–2) (1996) 185–204.
[45] U. Pliquett, S. Gallo, S.W. Hui, C. Gusbeth, E. Neumann, Local and transient structural changes in stratum corneum at high electric fields: contribution of Joule heating, Bioelectrochemistry 67 (1) (2005) 37–46.
[46] T.J. Franz, Percutaneous absorption. On the relevance of in vitro data, J. Investig. Dermatol. 64 (3) (1975) 190–195.
[47] Lusiana, S. Reichl, C.C. Müller-Goymann, Keratin film made of human hair as a nail plate model for studying drug permeation, Eur. J. Pharm. Biopharm. 78 (3) (2011) 432–440.
[48] J. Fokuhl, C.C. Müller-Goymann, Untersuchung der Unversehrtheit von humanem exzidiertem Stratum corneum mittels TEER-Messungen, Erlangen, Germany, September 10-13th, 2007.
[49] J.W. Fluhr, S. Sassning, O. Lademann, M.E. Darvin, S. Schanzer, A. Kramer, H. Richter, W. Sterry, J. Lademann, In vivo skin treatment with tissue-tolerable plasma influences skin physiology and antioxidant profile in human stratum corneum, Exp. Dermatol. 21 (2) (2012) 130–134.
[50] P. Rajasekaran, P. Mertmann, N. Bibinov, D. Wandke, W. Viöl, P. Awakowicz, Filamentary and homogeneous modes of dielectric barrier discharge (DBD) in air: investigation through plasma characterization and simulation of surface irradiation, Plasma Process. Polym. 7 (8) (2010) 665–675.
[51] M.L. Thomson, A comparison between the number and distribution of functioning eccrine sweat glands in Europeans and Africans*, J. Physiol. 123 (2) (1954) 225–233.
[52] H.E. Boddé, I. van den Brink, H.K. Koerten, F.H.N. de Haan, Visualization of in vitro percutaneous penetration of mercuric chloride; transport through intercellular space versus cellular uptake through desmosomes, J. Control. Release 15 (3) (1991) 227–236.
[53] I. Plasencia, L. Norlén, L.A. Bagatolli, Direct visualization of lipid domains in human skin stratum corneum's lipid membranes: effect of pH and temperature, Biophys. J. 93 (9) (2007) 3142–3155.
[54] M. Yusupov, J. Van der Paal, E.C. Neyts, A. Bogaerts, Synergistic effect of electric field and lipid oxidation on the permeability of cell membranes, Biochim. Biophys. Acta - Gen. Subj. 1861 (4) (2017) 839–847.
[55] J. Lademann, A. Patzelt, H. Richter, O. Lademann, G. Baier, L. Breucker, K. Landfester, Nanocapsules for drug delivery through the skin barrier by tissue-tolerable plasma, Laser Phys. Lett. 10 (8) (2013) 83001.